RSC Advances




ROYAL SOCIETY OF CHEMISTRY

www.rsc.org/advances

# Adsorption of Cd(II) from aqueous solution by biogenic selenium nanoparticles

Fanghui Yuan, Chao Song, Xuefei Sun, Linrui Tan, Yunkun Wang, Shuguang Wang*

Shandong Key Laboratory of Water Pollution Control and Resource Reuse, School of Environmental Science and Engineering, Shandong University, Jinan 250100, China

Corresponding author:

E-mail: wsg@sdu.edu.cn; Tel: +86 531 88365919; Fax: +86 531 88364513

## Abstract

Biogenic selenium nanoparticles (BioSeNPs), which were produced by aerobic granular sludge in a sequencing batch reactor (SBR), were used to remove cadmium from aqueous solution. Batch experiments were carried out to investigate the effect of contact time, initial solution pH and adsorbent dosage on adsorption. Langmuir model was more suitable to describe the adsorption process than Freundlich model with the monolayer maximum adsorption capacity of 59.7 mg/g for Cd(II) adsorption by BioSeNPs. The isotherm data were also well described by the Temkin model, which further supported that Cd(II) adsorption was a chemisorption process. The adsorption kinetics data were well described by the pseudo-second-order kinetic model with $r^2$ values exceeding 0.999. The overall rate process was influenced by both external mass transfer and intra particle diffusion, but was mainly controlled by intra particle diffusion. The negative values of $\Delta G^0$ and $\Delta H^0$ indicated that the adsorption process was spontaneous and exothermic. Energy dispersive X-ray spectrometry (EDS) analysis confirmed that Cd(II) was adsorbed onto BioSeNPs. After loaded with Cd(II), the BioSeNPs had less negative zeta potential values and no obvious change in the iso-electric point was observed. The Fourier transform infrared spectroscopy (FTIR) and X-ray photoelectron spectroscopy (XPS) spectra analysis indicated that the removal of Cd(II) was a complicated process, in which electrostatic attraction and surface complex formation were involved. The results demonstrated that BioSeNPs could be used to remove cadmium from aqueous solution with high efficiency.


**Keywords:** BioSeNPs; Cadmium; Adsorption; XPS; FTIR; Mechanisms

## Introduction

Due to the fast development of the industry in recent decades, more and more heavy metals were emitted into the environment[1-3]. Those metals are usually highly toxic, nonbiodegradable, carcinogenicity and can be accumulated through the food chain even in very low concentrations[4]. Therefore, it is urgent and necessary to remove heavy metals from natural waters.

Cadmium (Cd) is one of those dangerous metals which is released into the environment through metal production, electroplating, photography and the manufacturing of batteries[5]. It has been reported that chronic exposure to Cd could lead to renal degradation, skeletal deformity, muscular cramps and death in mammals and humans[4]. Thus, the UK Department of Environment has listed Cd in the red list of priority pollutants and it also has been included in the black list of Dangerous Substance Directive in European Economic Community[3]. According to the previous researches, there are many methods for Cd removal from wastewater including chemical precipitation, coagulation-flocculation, membrane filtration, ion exchange, electrolysis and adsorption[1]. Compared with the other methods, adsorption is more flexible and easy to operate, with low operational cost and high efficient in the removal of heavy metal ions from dilute solutions[6]. Various adsorbents such as activated carbon[7], root cell walls[8] and bamboo charcoal[3] have been studied in recent decades. However, those adsorbents are usually inefficiency. It is still a long way to search for adsorbents with higher adsorption capacity, faster kinetics and lower cost.

In recent years, the application of selenium nanoparticles (SeNPs) has attracted great attention. Previous studies have reported that SeNPs could be utilized as antimicrobials, fertilizers, semiconductors and sensors[9]. Recently, it was found that SeNPs could be used as adsorbent for the removal of heavy metals in solution due to its small size, large specific surface area and negative

surface charge[6]. Although chemically produced selenium nanoparticles (CheSeNPs) adsorb high quantities of copper[10], chemical production methods are costly and not environment-friendly due to the use of toxic reagents, high temperature and high pressure. In contrast, SeNPs, especially the biologically produced selenium nanoparticles (BioSeNPs), can be a potential adsorbent for heavy metal cations such as zinc, copper and nickel[6] because they can be produced by an eco-friendly method under ambient conditions. BioSeNPs produced by the anaerobic reduction of selenite in presence of anaerobic granules sludge have been successfully used to remove zinc from water system. Compared with the anaerobic granules sludge, aerobic granular sludge has attracted more attention due to its advantages such as short start time, perfect ability in biological removal of nitrogen and phosphorus. However, there is no information about using aerobic biologically produced SeNPs as an adsorbent so far. If BioSeNPs were produced by aerobic granular sludge in a sequencing batch reactor (SBR), it may provide a promising way for treating wastewaters which contain heavy metals and selenium oxyanions.

The present study investigated the feasibility of BioSeNPs which was first produced by aerobic granular sludge to remove Cd(II) from wastewaters. The adsorption characteristics of Cd(II) onto BioSeNPs were investigated under varying experimental conditions, such as contact time, initial solution pH and adsorbent dosage. The adsorption kinetics and isotherm data, as well as Fourier transform infrared spectroscopy (FTIR) and X-ray photoelectron spectroscopy (XPS) analysis, were processed to understand the adsorption mechanism. This study would provide an overall understanding for the Cd(II) adsorption by BioSeNPs.

## Materials and methods

### Selenium nanoparticles production and purification

Selenium nanoparticles were produced by aerobic granular sludge in a SBR with an initial mixed

liquor suspended solids (MLSS) concentration of 3,000 mg/L and sludge volume index (SVI) of 33.6 mL/g. The SBR was operated at room temperature (22-25$^{o}$C) and neutral pH (7.2-7.5). Sodium selenite was added as selenium source.

The production of SeNPs were confirmed by the appearance of a red color both on the granular sludge and in the medium[11]. The effluent was collected by simple decanting and then was concentrated by centrifuging at 5,000 rpm and 4$^{o}$C. The pellet was re-suspended in distilled water and purified by the protocol described by Jain et al[6]. The obtained pellet was lyophilized and stored in drying vessel at room temperature.

**Characterization of the BioSeNPs**

The surface morphology and size of the BioSeNPs were characterized by Scanning Electron Microscope (SEM, JSM 6700F, JEOL, Japan). Energy dispersive X-ray spectrometry (EDS, Oxford, INCA X sight, OIMS, England) was used to analyze the elemental composition of the BioSeNPs before and after Cd(II) adsorption. The average particle size of the BioSeNPs was measured by dynamic light scattering (DLS, BI-200SM/BI-9000, Brookhaven Instrument Co., USA).The iso-electric point (IEP) of BioSeNPs was measured by a laser electrophoresis zeta potential analyzer (Zetasizer III, Malvern, USA).

FTIR (Bruker Tensor 27 spectrometer, USA) was also used to analyze of the dried BioSeNPs samples before and after Cd(II) adsorption. The XPS (Thermo ESCALAB 250, USA) spectra of the BioSeNPs before and after Cd(II) adsorption were collected applying the energy source of monochromatic Al *Kα* radiation (1486.6 eV) operated at 150 W. The wide scans were conducted from 0 to 1200 eV with pass energy of 70 eV. The elements to be analyzed were scanned over different energy ranges with the pass energy of 30 eV. The binding energy of the spectra was standardized with the C 1s

peak at 284.8 eV.

**Preparation of solutions**

All the chemicals used in this study were of guaranteed analytical grade purchased from Sinopharm (Shanghai, China). The stock solution of Cd(II) with a concentration of 20 g/L was prepared by dissolving Cd $(NO_3)_2 \cdot 4H_2O$ in deionized water. The desired Cd(II) concentrations in latter experiments were prepared by diluting stock solution with deionized water.

**Batch adsorption experiments**

Adsorption experiments were performed in a thermo forma orbital shaker with shaking speed of 160 rpm at 30$^{o}$C. A series of adsorption experiments were carried out in 50 mL conical flasks which contained 20 mL Cd(II) solution at the required concentration and pH. Time-dependency studies were carried out at pH 7.0 with the Cd(II) and BioSeNPs concentration of 50 mg/L and 1.0 g/L, respectively. The samples were collected at different time intervals up to 24 h to determine the equilibrium time. Single-point adsorption experiments were carried out to investigate the effect of initial solution pH on the adsorption process. The initial Cd(II) concentration was 50 mg/L and the pH values of initial solutions were adjusted in the range of 4.0-10.0 with HCl (0.1 M) or NaOH (0.1 M) solutions. Control experiments were carried out to rule out the influence of precipitation. The effect of adsorbent dosage at pH 7.0 was studied by varying the adsorbent dosage (0.5–5.0 g/L) with the initial Cd(II) concentration in the range of 20-100 mg/L.

**Adsorption kinetics experiments**

Adsorption kinetics experiments were carried out with three different initial Cd(II) concentrations of 20, 50 and 100 mg/L, respectively. The pH was set at 7.0 and the adsorbent concentration was set at 1.0 g/L. Samples were collected at 0, 0.5, 1, 2, 4, 6, 9, 12 and 15 h for Cd(II) analysis.

**Adsorption isotherm experiments**

Cd(II) solutions with various concentrations (10-150 mg/L) were added to 50 mL conical flasks for adsorption experiments. Then, a certain amount of BioSeNPs was added into each flask making the concentration at 1.0 g/L. Those flasks were stirred at 160 rpm under five temperatures (293, 298, 303 308 and 313 K) for 10 h to reach the adsorption equilibrium. The samples were collected at 0 and 10 h to quantify the initial and the equilibrium Cd(II) concentrations.

The obtained samples were first centrifuged at 8,000 rpm for 10 min, and then the supernatant was filtered with 0.22 μm syringe filters. The residual Cd(II) concentration in filtrate was analyzed by flame Atomic Absorption Spectrophotometer. Control experiments were carried out to discard the possibility of adsorption of Cd (II) ions to the filter material and conical flasks.

The adsorption capacity was expressed as amount of Cd(II) adsorbed per mass unit of BioSeNPs using the following equation:

$$q_e = \frac{C_0 - C_e}{C_a} \quad (1)$$

where $C_0$ is the initial Cd(II) concentration (mg/L), $C_e$ is the final or equilibrium Cd(II) concentration (mg/L), and the $C_a$ is the concentration of BioSeNPs (mg/L).

## Results and discussion

**Characterization of the BioSeNPs**

The red BioSeNPs synthesized by the reduction of $SeO_3^{2-}$ by aerobic granular sludge are primarily spherical in shape with the size in the range of 50-150 nm (Fig. S1). EDS analysis of the BioSeNPs indicated the presence of selenium (Fig. 1a). The presence of carbon, oxygen, phosphorus and sulfur may response to the presence of extracellular polymeric substances (EPS) which attached to the BioSeNPs. EDS analysis of the Cd-loaded BioSeNPs confirmed the existence of Cd(II). The

characteristic peak for Cd was at 3.20 Kev which was similar to the Cd(II) signal observed at the same energy in the Cd-loaded nZVI particles[12]. The DLS analysis of BioSeNPs solution revealed that particles were in the size range of 98 nm to 131 nm with an average size of 113 nm (Fig. 1b) which was in agreement with the SEM finding. The polydispersity index (PDI) was 0.005, indicating high stability of BioSeNPs in solution[13].

As shown in Fig. 2, the IEP of BioSeNPs was at pH 4.1. Above pH 6.0, BioSeNPs suspensions were colloidally stable due to their intrinsic negative charge of $< -25$ mV[14]. Hence, BioSeNPs have a potential ability to combine with heavy metal cations. After loaded with Cd(II), the BioSeNPs has less negative zeta potential values especially at alkaline pH due to the combination of anion-cation, suggesting that the colloidal stability of BioSeNPs decreased after Cd(II) loaded on the surface of BioSeNPs. No appreciable change was observed in the IEP, this can be accounted for the relatively small amount of Cd(II) adsorption at pH 4.1.

**Batch adsorption experiments**

*Effect of contact time*

The result in Fig. 3 shows that the adsorption capacity increased quickly in the first two hours and about half of total Cd(II) were adsorbed in 15 min. In the following 6 h, the adsorption capacity still increased but with a slow rate than before. The adsorption process was completed within 8 h and remained unchanged for longer contact time. Thus, all further experiments were carried out for 10 h to ensure adsorption equilibrium was achieved.

*Effect of initial solution pH*

Initial solution pH is an important factor in the adsorption process because it affects the existence form of the metal ions and the adsorption capacity of the adsorbent. Precipitation occurring at alkaline

environment masks the true extent of metal adsorption on adsorbent. To exclude the influence of precipitation on adsorption capacity, control experiment without BioSeNPs added was carried out to evaluate the effects of pH on soluble Cd(II) concentration and the results were shown in Fig. 4. It was found that the Cd(II) concentration almost unchanged in the pH range of 4.0 - 7.5, indicating no Cd(II) precipitation happened under those pH values. When pH was higher than 7.5, the residual concentration (R.C) of the Cd(II) in solution decreased due to the precipitation. Therefore, pH ranged from 4.0 to 7.5 were chosen to make sure that the decrease of Cd(II) concentration is only attributed to adsorption. The adsorption capacity of adsorbents increased with increasing pH from 4.0 to 7.5, which is consistent with the previous studies[2, 3, 15, 16]. One possible reason is that higher concentration of $H^+$ in the solution would compete with Cd(II) for the adsorption sites, leading to the reduced uptake[17]. Another reason is that the surface charge of BioSeNPs changed under different pH values. As mentioned in the zeta potential analysis, the BioSeNPs have an IEP at pH 4.1, the negative charge increased from 0 to -40 mV with increasing pH from 4.1 to 7.5, which favored the adsorption of the positively charged Cd(II). Therefore, it can be concluded that electrostatic attraction plays an important role in the adsorption of Cd(II) by BioSeNPs.

*Effect of BioSeNPs dosage*

Adsorbent concentration is an important factor in an adsorption process, because it determines the availability of active sites which influences the adsorption capacity of the adsorbent. As shown in Fig. 5a, the removal efficiency first increased rapidly with the increasing adsorbent dosage, which can be attributed to the more available adsorption sites provided by the higher concentration of adsorbents[1]. However, once almost all Cd(II) is adsorbed, the removal efficiency had no obvious increase with the increased adsorbent concentration. It could be explained that the adsorption process reached the point

where surface metal ions concentration and the solution metal ions concentration come to equilibrium with each other[18].

As shown in Fig. 5b, adsorption capacity, the amount of Cd(II) adsorbed per mass unit of BioSeNPs, decreased with the increasing adsorbent dosage. One possible explanation is that the available Cd(II) concentration is insufficient to cover the active sites at high adsorbent concentrations, resulting in low metal uptake[19]. Another explanation is that high adsorbent concentration will cause particle–particle aggregation and lead to a decrease of the total surface area which cause decreased adsorption[17]. Adsorption capacity increased with increasing initial Cd(II) concentration of solution and the increased $q_e$ at higher initial concentration can be attributed to enhanced driving force[3].

**Adsorption kinetics**

The kinetics of adsorption would help to understand the adsorption mechanisms and investigate the efficiency of adsorbent for the removal of pollutants[20]. In this study, in order to evaluate the kinetics of the adsorption process, the pseudo-first-order, pseudo-second-order and intra particle diffusion models were used to analyze the experimental data.

The liner form of pseudo-first-order model[12] is expressed as:

$$\log(q_e - q_t) = \log q_e - \frac{k_1}{2.303} t \quad (2)$$

where $k_1$ ($s^{-1}$) is the pseudo-first-order rate constant, which can be calculated by plotting $\log(q_e - q_t)$ versus t.

The linear form of pseudo-second-order model[12] can be expressed as:

$$\frac{t}{q_t} = \frac{1}{k_2 q_e^{\,2}} + \frac{1}{q_e} t \quad (3)$$

where $k_2$ (g/mg s) is the rate constant of the pseudo-second-order adsorption, which can be calculated by plotting $t/q_t$ versus t.

The intra particle diffusion model is expressed as[21]:

$$q_t = k_{id} t^{0.5} + I \quad (4)$$

where $k_{id}$ is the intra particle diffusion rate constant (mg $g^{-1}$ $h^{0.5}$) and I is the intercept (mg/g), which can be calculated by plotting $q_t$ versus $t^{0.5}$.

Fig. 6a shows the pseudo-first-order kinetic plots between $\log(q_e - q_t)$ versus t for Cd(II) adsorption at different initial metal concentrations. Kinetic parameters including the first-order rate constant ($k_1$), calculated equilibrium adsorption capacity ($q_{e,cal}$) and the regression coefficients ($r^2$) were calculated and summarized in Table 1. The much difference between $q_{e,exp}$ and $q_{e,cal}$ and also the much lower regression coefficients ($r^2$<0.92) indicated that the pseudo-first-order model is not appropriate to describe the adsorption of Cd(II) onto BioSeNPs.

Fig. 6b shows the pseudo-second-order kinetic plots between $t/q_t$ versus t for Cd(II) adsorption at different initial metal concentrations and the obtained kinetic parameters were shown in Table 2. All the three regression coefficients ($r^2$) were higher than 0.999, suggesting the adsorption process follows the pseudo-second-order kinetics. Moreover, the theoretical $q_e$ calculated from the pseudo-second-order kinetic model were in good agreement with those obtained experimentally, which also suggested that the pseudo-second-order model is more suitable for representing Cd(II) adsorption kinetics on BioSeNPs.

In order to identify the diffusion mechanism, the intra particle diffusion model was used to predict the rate-controlling step. From this study, multi-linearities were observed (Fig. 6c), indicating that there was three-stage diffusion of Cd(II) onto BioSeNPs. The first stage was from 0 h to 1 h, representing external mass transfer. The second stage included the adsorption period from 1 h to 8 h, representing intra particle diffusion. The last stage indicated adsorption–desorption equilibrium, including the period

229 from 8 h to 12 h[15].

230 Kinetic parameters ($k_{id}$ and I) of the intra particle diffusion section were calculated and
231 summarized in Table 3. As the plots did not pass through the origin, intra particle diffusion is not the
232 unique rate-controlling step[15]. Due to the large intercepts of the second linear portion of the plots, the
233 external mass transfer is also significant in the rate-controlling step[22]. However, the ratio of the time
234 taken by external mass transfer to intra particle diffusion was about 1:7. So intra particle diffusion was
235 predominated over the external mass transfer.

236 **Adsorption isotherms**

237 Adsorption isotherms describe the adsorption mechanism of a solute adsorb on adsorbent surface
238 which helps in optimizing the design of a specific adsorption process. In this study, the equilibrium
239 data obtained for Cd removal using BioSeNPs were tested with three isotherm models available in the
240 literature to reveal the best fitting isotherm[5].

241 The Freundlich isotherm is applicable to describe the adsorption of metal occurs on a
242 heterogeneous surface by multilayer adsorption. The linear form of Freundlich isotherm equation[12] is
243 expressed as:

244 $$\log q_e = \log K_F + \frac{1}{n} \log C_e \quad (5)$$

245 where $K_F$ and n are Freundlich isotherm constants which can be obtained from the plot of $\log q_e$ versus
246 $\log C_e$ on the basis of the linear form of Freundlich equation. Those constants are also related to
247 adsorption capacity and adsorption intensity, respectively. $C_e$ is the equilibrium concentration (mg/L).

248 The Langmuir isotherm assumes monolayer adsorption on a homogeneous surface with a finite
249 number of adsorption sites. After a certain time, the surface will eventually reach a saturation point and
250 achieve the maximum adsorption. The linear form of the Langmuir isotherm model[12] is described as:

$$\frac{C_e}{q_e} = \frac{1}{K_L q_m} + \frac{C_e}{q_m} \quad (6)$$

where $K_L$ is the Langmuir constant related to the rate of adsorption and $q_m$ is the maximum adsorption capacity (mg/g)[12].

The Langmuir constant, ($K_L$) is adapted to calculate the dimensionless separation factor ($R_L$), which determines the favorability of the adsorption process. The relationship between $R_L$ and $K_L$ can be expressed as[20]:

$$R_L = \frac{1}{1 + K_L C_0} \quad (7)$$

where $C_0$ is the initial concentration. $R_L$ value indicates whether the isotherm is favorable ($0<R_L<1$), linear ($R_L=1$), unfavorable ($R_L > 1$), or irreversible ($R_L = 0$).

The Temkin isotherm model assumes that the adsorption energy would decrease linearly with the surface coverage due to adsorbent-adsorbate interactions. The linear form of Temkin isotherm model[12] is given as:

$$q_e = \frac{RT}{b} \ln K_T + \frac{RT}{b} \ln C_e \quad (8)$$

where T is the absolute temperature in Kelvin and R is the universal gas constant, b (J/mol) is the Temkin constant related to the heat of adsorption and $K_T$ (L/mg) is the equilibrium binding constant corresponding to the maximum binding energy, both b and $K_T$ can be obtained from the plot of $q_e$ versus ln $C_e$ on the basis of the linear form of Temkin isotherm[12].

The adsorption studies were conducted at a fixed initial concentration of Cd(II) by changing temperature. The equilibrium data obtained from the isotherm studies were fitted to Freundlich, Langmuir and Temkin isotherm models to obtain the best fitting isotherm. The isotherms were shown graphically in Fig. 7 and the isotherm parameters were listed in Table 4. As shown in Table 4, the value

of $K_F$ decreased with the increasing of temperature, which indicated the adsorption process of Cd(II) onto BioSeNPs is exothermic.

According to the results, both Langmuir model and Temkin model were suitable to describe this adsorption process with high linearity coefficients. Comparison of coefficients indicates that the Langmuir isotherm fitted more precisely ($r^2 > 0.97$) than the Temkin isotherm ($r^2 > 0.95$). The basic assumption of Langmuir adsorption isotherm is monolayer adsorption on a homogenous surface with a finite number of adsorption sites, which means that the adsorption of Cd(II) onto BioSeNPs generates monolayer formation[3]. The maximum adsorption capacity was 59.7 mg/g and it is much higher than most other adsorbents reported in the previous literatures: bamboo charcoal (12.08 mg/g)[3], activated guava leaves (19.15 mg/g)[4], $MnO_2$ functionalized multi-walled carbon nanotubes (41.6 mg/g)[15], modified algae (41.80 mg/g)[23], activated alumina (35.06 mg/g)[18], untreated *Pinus halepensis* sawdust (7.35 mg/g)[5], porous urea–formaldehyde (3.12 mg/g)[24], wheat stem (11.16 mg/g)[25]. The calculated values of $R_L$ for the adsorbent at different temperatures are 0.23 (293 K), 0.25 (303 K), and 0.31 (313K). All the values of $R_L$ are less than unity, which confirms the favorable adsorption process. The basic assumption of Temkin adsorption isotherm is chemisorption process and the linear plots for Temkin adsorption isotherm fit quite well with $r^2 > 0.95$ under all temperatures. This indicated that the adsorption of Cd(II) onto BioSeNPs is a chemisorption process[12].

**Thermodynamic Parameters**

Temperature dependence of the adsorption process is associated with several thermodynamic parameters such as Gibb's free energy change ($\Delta G^0$), enthalpy change ($\Delta H^0$) and change in entropy ($\Delta S^0$), which can be determined by using the following equations[20]:

$$\Delta G^0 = -RT\ln(\frac{q_e}{C_e}) \quad (9)$$

$$\ln\left(\frac{q_e}{C_e}\right) = \frac{\Delta S^0}{R} - \frac{\Delta H^0}{RT} \quad (10)$$

The values of $\Delta H^0$ and $\Delta S^0$ can be calculated by plotting $\ln(q_e/C_e)$ versus 1/T (Fig. 8). All those thermodynamic parameters for adsorption of Cd(II) by BioSeNPs were shown in Table 5.

As shown in Table 5, the negative values of $\Delta G^0$ indicate that the adsorption processes are spontaneous at the studied temperatures. However, the increase in temperature lead to a less negative value of $\Delta G^0$, indicating that the reaction becomes less spontaneous at high temperatures. This is confirmed by the negative value of $\Delta H^0$, which revealed that the adsorption of Cd(II) on BioSeNPs is an exothermic process. The negative values of $\Delta S^0$ suggested there is a decrease in the randomness at solid–liquid interface of Cd(II) onto BioSeNPs surface and no significant changes occur in the internal structure of the adsorbent through the adsorption. Similar results for thermodynamic parameters were also reported by the earlier workers for the adsorption of Cd(II) as well as other heavy metals from aqueous solution[17].

**Adsorption mechanism**

The FTIR spectra of BioSeNPs and Cd-loaded BioSeNPs in the range of 750 – 3750 $cm^{-1}$ are shown in Fig. 9. The characteristic absorption peaks for BioSeNPs are summarized as follows[26]: peak at 3298 $cm^{-1}$ is related to N-H stretching vibrations of amine; peak at 2932 $cm^{-1}$ is attributed to C-H stretching of aliphatic; peak at 1655 $cm^{-1}$ mainly represents the stretching vibration of C=O present in proteins (amide I); peak at 1540 $cm^{-1}$ corresponds to the N−H bending vibration in amide linkage of proteins (amide II); the peak at 1387 $cm^{-1}$ is most likely attributed to the $-CH_3$ umbrella mode in aliphatic or O-H in-plane bending in carbohydrates; peak at 1054 $cm^{-1}$ is related to C−O−C stretching arising from the carbohydrate groups. The presence of carboxylic groups is also evidenced by the peak observed at 1726 $cm^{-1}$. The FTIR of Cd-load BioSeNPs had all the key features of original BioSeNPs

316 with minor shifts and changes in peak intensities. When Cd(II) were adsorbed on the BioSeNPs, peak
317 at 3298 $cm^{-1}$ shifted to 3288 $cm^{-1}$; 1655 $cm^{-1}$ shifted to 1644 $cm^{-1}$; 1540 $cm^{-1}$ shifted 1530 $cm^{-1}$,
318 respectively. Shifts in these peaks indicated that Cd(II) reacted with the function groups (C=O, N-H,
319 C-N) of BioSeNPs.

320 The XPS analysis was applied to characterize the function groups involved in the adsorption
321 process. The general spectra for BioSeNPs before and after adsorption are present in Fig. S2. The scan
322 spectra showed the presence of C 1s, O 1s, N 1s, Se 3d and Cd 3d signals. The presence of C 1s, O 1s
323 and N 1s signals may attribute to the existence of protein generated during BioSeNPs production[27], and
324 the presence of protein was also provided by the UV-vis spectrum of BioSeNPs (Fig. S3). Cd 3d signal
325 was observed after adsorption which proved the existence of Cd on BioSeNPs. The signal can be
326 resolved into two peaks with binding energies located at 404.76 eV and 405.40 eV, corresponding to
327 CdO and $Cd(OH)_2$[16]. However, the Se 3d signal was very weak, which might be attributed to the
328 proteins coating on BioSeNPs[27].

329 As shown in Fig. 10a-d, the signals of C 1s, O 1s did not show any significant shift before and
330 after adsorption. The C 1s signal can be divided into three peaks with binding energies located at 284.6,
331 285.9 and 287.7 eV corresponded to C-(C, H), C-(C, N), and C=O groups, respectively[28]. The O 1s
332 signal can be assigned to three peaks with binding energies located at 530.4, 531.3 and 532.2 eV,
333 corresponding to C-OH, C=O, and C-O groups[2]. As shown in Fig. S4, the binding energy for N 1s is
334 centered at 399.5 eV and it may correspond to nitrogen containing groups such as amine and amide
335 groups[6].

336 The relative contents of C and O in different groups on the surface of BioSeNPs before and after
337 Cd(II) adsorption are summarized in Table 6. From the relative contents of oxygen, the content of C-O

groups decreased from 38.1% to 29.9% after Cd adsorption, while the amount of C=O groups increased from 33.4% to 40.6%. From the relative contents of carbon, the content of C=O groups increased from 6.9% to 7.5%, which was consistent with the finding from the relative contents of oxygen. The changes of C-O and C=O groups suggested that these groups were involved in the adsorption of Cd(II) onto BioSeNPs, which was in accordance with the FTIR analysis. The decrease of C-O groups after Cd adsorption indicated the formation of Cd-O complex species[2], which was supported by the findings we obtained in the XPS spectra of Cd 3d (Fig. 10g).

As shown in Fig. 10e-f, the signals of the Se 3d showed a little shift before and after adsorption. The Se $3d_{5/2}$ peaks at 55.88 eV, 56.75 eV shifted to 56.26 eV, 57.08 eV, respectively[6]. It may be explained as that Cd(II) adhered on the surface of the negatively charged BioSeNPs by the electrostatic attraction[10] and attributed to the formation of Se-Cd complexes.

## Conclusions

The removal of Cd(II) metal ions from aqueous solution by BioSeNPs was investigated. The adsorption capacity increased with the increasing solution pH and decreased with the increasing adsorbent dosage. EDS analysis confirmed that Cd(II) was adsorbed onto BioSeNPs. After loaded with Cd(II), the BioSeNPs had less negative zeta potential values and no appreciable change in the IEP. Langmuir model was more suitable to describe the adsorption process than Freundlich model isotherm. The obtained monolayer maximum adsorption capacity was 59.7 mg/g for the adsorption of Cd(II) by BioSeNPs. The equilibrium data were also well described by the Temkin model isotherm, supporting that Cd(II) adsorption was a chemisorptions process. The kinetics of Cd(II) adsorption onto BioSeNPs was accurately described by the pseudo-second-order kinetic model with $r^2$ values exceeding 0.999. The overall rate process was influenced by both external mass transfer and intra particle diffusion, but

was mainly controlled by intra particle diffusion. The negative values of $\Delta G^0$ and $\Delta H^0$ indicate that the adsorption process was spontaneous and exothermic. The removal of Cd(II) was a complicated process, in which electrostatic attraction and surface complex formation were involved. Because BioSeNPs were produced by aerobic granular sludge in a SBR, this may provide a new way for treating wastewaters which contain heavy metals and selenium oxyanions.

## Acknowledgements

This research was funded by the National Natural Science Foundation of China (51178254 and 51208283), Research Award Fund for Outstanding Young Scientists of Shandong Province, China (BS2012HZ008) and China Postdoctoral Science Foundation (2015M570596).

## References

1. L. Zeng, Y. Chen, Q. Zhang, X. Guo, Y. Peng, H. Xiao, X. Chen and J. Luo, *Carbohydrate Polymers*, 2015, **130**, 333-343.
2. Q. Li, L. Chai and W. Qin, *Chemical Engineering Journal*, 2012, **197**, 173-180.
3. F. Y. Wang, H. Wang and J. W. Ma, *Journal of Hazardous Materials*, 2010, **177**, 300-306.
4. O. Abdelwahab, Y. O. Fouad, N. K. Amin and H. Mandor, *Environmental Progress & Sustainable Energy*, 2015, **34**, 351-358.
5. L. Semerjian, *Journal of Hazardous Materials*, 2010, **173**, 236-242.
6. R. Jain, N. Jordan, D. Schild, E. D. van Hullebusch, S. Weiss, C. Franzen, F. Farges, R. Hübner and P. N. L. Lens, *Chemical Engineering Journal*, 2015, **260**, 855-863.
7. H. K. An, B. Y. Park and D. S. Kim, *Water Research*, 2001, **35**, 3551-3556.
8. G. Chen, Y. Liu, R. Wang, J. Zhang and G. Owens, *Environmental Science and Pollution Research*, 2013, **20**, 5665-5672.

9. Y. V. Nancharaiah and P. N. L. Lens, *Trends in Biotechnology*, 2015, **33**, 323-330.

10. Y. Bai, F. Rong, H. Wang, Y. Zhou, X. Xie and J. Teng, *Journal of Chemical & Engineering Data*, 2011, **56**, 2563-2568.

11. W. Zhang, Z. Chen, H. Liu, L. Zhang, P. Gao and D. Li, *Colloids and Surfaces B: Biointerfaces*, 2011, **88**, 196-201.

12. H. K. Boparai, M. Joseph and D. M. O'Carroll, *Journal of Hazardous Materials*, 2011, **186**, 458-465.

13. N. Srivastava and M. Mukhopadhyay, *Powder Technology*, 2013, **244**, 26-29.

14. B. Buchs, M. W. H. Evangelou, L. H. E. Winkel and M. Lenz, *Environmental Science & Technology*, 2013, **47**, 2401-2407.

15. C. Luo, R. Wei, D. Guo, S. Zhang and S. Yan, *Chemical Engineering Journal*, 2013, **225**, 406-415.

16. L. Peng, Q. Zeng, B. Tie, M. Lei, J. Yang, S. Luo and Z. Song, *Journal of Colloid and Interface Science*, 2015, **456**, 108-115.

17. T. K. Sen and D. Gomez, *Desalination*, 2011, **267**, 286-294.

18. T. K. Naiya, A. K. Bhattacharya and S. K. Das, *Journal of Colloid and Interface Science*, 2009, **333**, 14-26.

19. S. Malamis and E. Katsou, *Journal of Hazardous Materials*, 2013, **252–253**, 428-461.

20. L. Cheng, L. Ye, D. Sun, T. Wu and Y. Li, *Chemical Engineering Journal*, 2015, **264**, 672-680.

21. S. A. Singh, B. Vemparala and G. Madras, *Journal of Environmental Chemical Engineering*, 2015, **3**, 2684-2696.

22. L. Zhang, T. Xu, X. Liu, Y. Zhang and H. Jin, *Journal of Hazardous Materials*, 2011, **197**,

389-396.

23. M. Harja, G. Buema, L. Bulgariu, D. Bulgariu, D. Sutiman and G. Ciobanu, *Korean Journal of Chemical Engineering*, 2015, **32**, 1804-1811.

24. C. Li, H. Duan, X. Wang, X. Meng and D. Qin, *Chemical Engineering Journal*, 2015, **262**, 250-259.

25. G. Tan and D. Xiao, *Journal of Hazardous Materials*, 2009, **164**, 1359-1363.

26. R. Jain, N. Jordan, S. Weiss, H. Foerstendorf, K. Heim, R. Kacker, R. Hübner, H. Kramer, E. D. van Hullebusch, F. Farges and P. N. L. Lens, *Environmental Science & Technology*, 2015, **49**, 1713-1720.

27. T. Wang, L. Yang, B. Zhang and J. Liu, *Colloids and Surfaces B: Biointerfaces*, 2010, **80**, 94-102.

28. C. Song, X.-F. Sun, S.-F. Xing, P.-F. Xia, Y.-J. Shi and S.-G. Wang, *Environmental Science and Pollution Research*, 2014, **21**, 1786-1795.

# Figure Captions

**Fig. 1** (a) EDS analysis of BioSeNPs and Cd-loaded BioSeNPs

(b) DLS analysis of BioSeNPs (avg. size: 113 nm)

**Fig. 2** Zeta potential measurements of BioSeNPs (a) and BioSeNPs exposed to 100 mg/L Cd(II) (b)

**Fig. 3** Effect of contact time on the adsorption of Cd(II) by BioSeNPs

**Fig. 4** Effect of initial solution pH on the adsorption of Cd(II) by BioSeNPs

**Fig. 5** Effect of BioSeNPs dosage on the adsorption of Cd(II) by BioSeNPs under different initial Cd(II) concentrations

**Fig. 6** Pseudo-first-order (a) Pseudo-second-order (b) Intra particle diffusion (c) kinetics of Cd(II) adsorption on BioSeNPs at various concentrations

**Fig. 7** Linearized Freundlich (a), Langmuir (b) and Temkin (c) isotherms for Cd(II) adsorption on BioSeNPs at different temperatures

**Fig. 8** Van't Hoff plot for adsorption of Cd(II) by BioSeNPs

**Fig. 9** FTIR spectra of BioSeNPs and Cd-loaded BioSeNPs

**Fig. 10** (a) C 1s (c) O 1s (e) Se 3d spectra of BioSeNPs and (b) C 1s (d) O 1s (f) Se 3d (g) Cd 3d spectra of Cd-loaded BioSeNPs

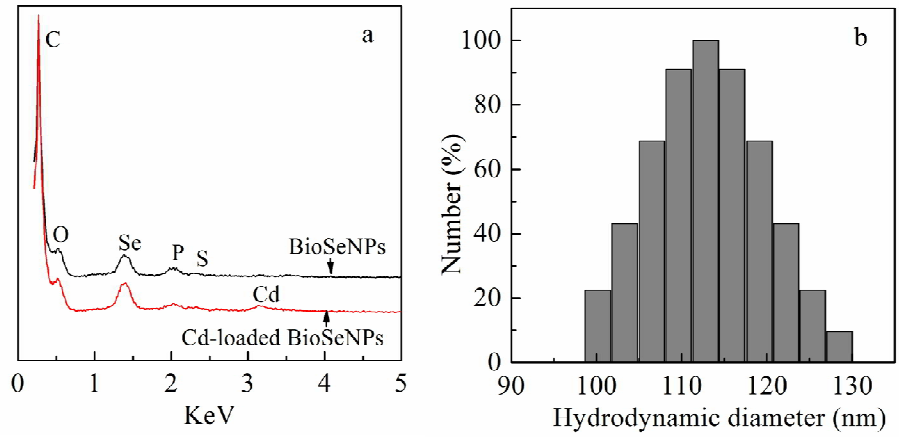


**Fig. 1**

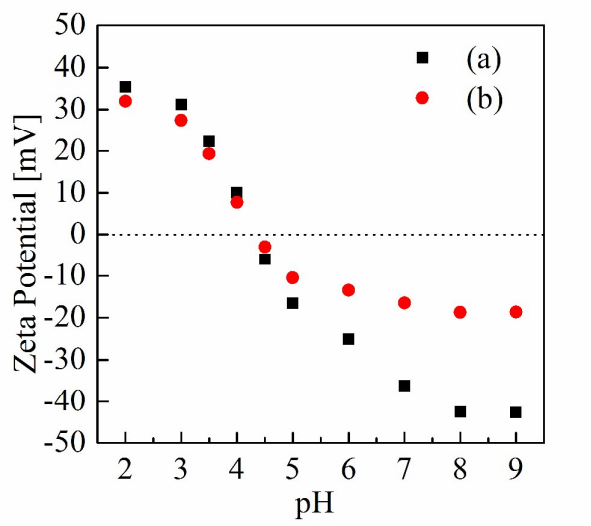


**Fig. 2**

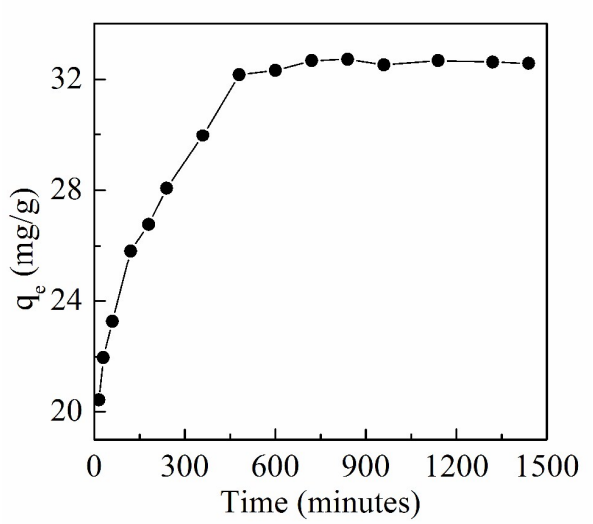


**Fig. 3**

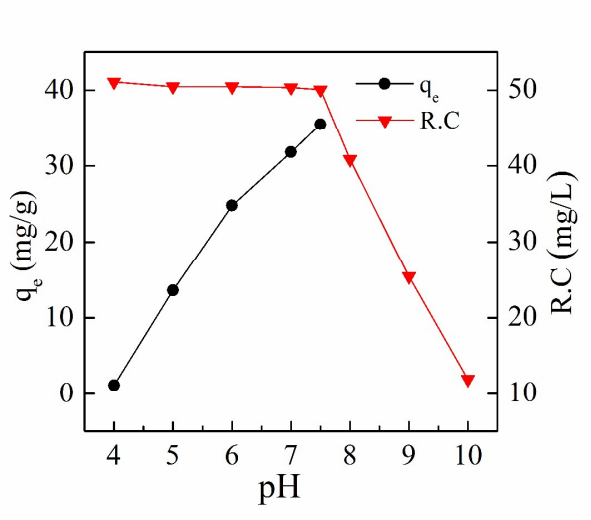


**Fig. 4**

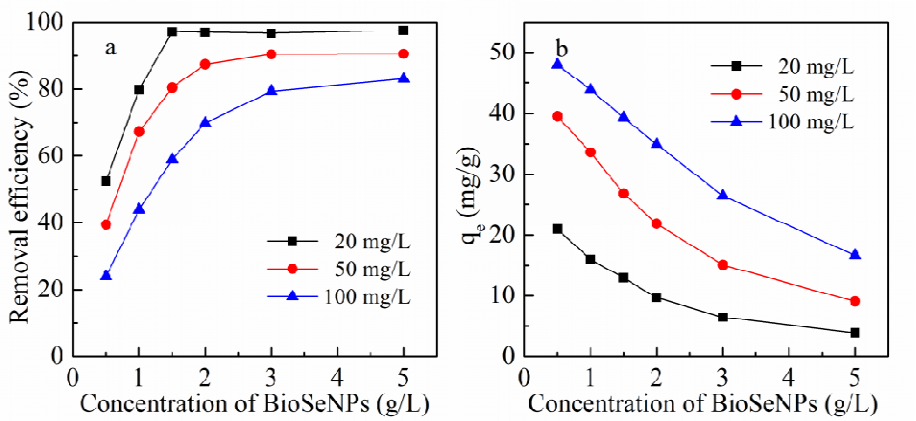


**Fig. 5**

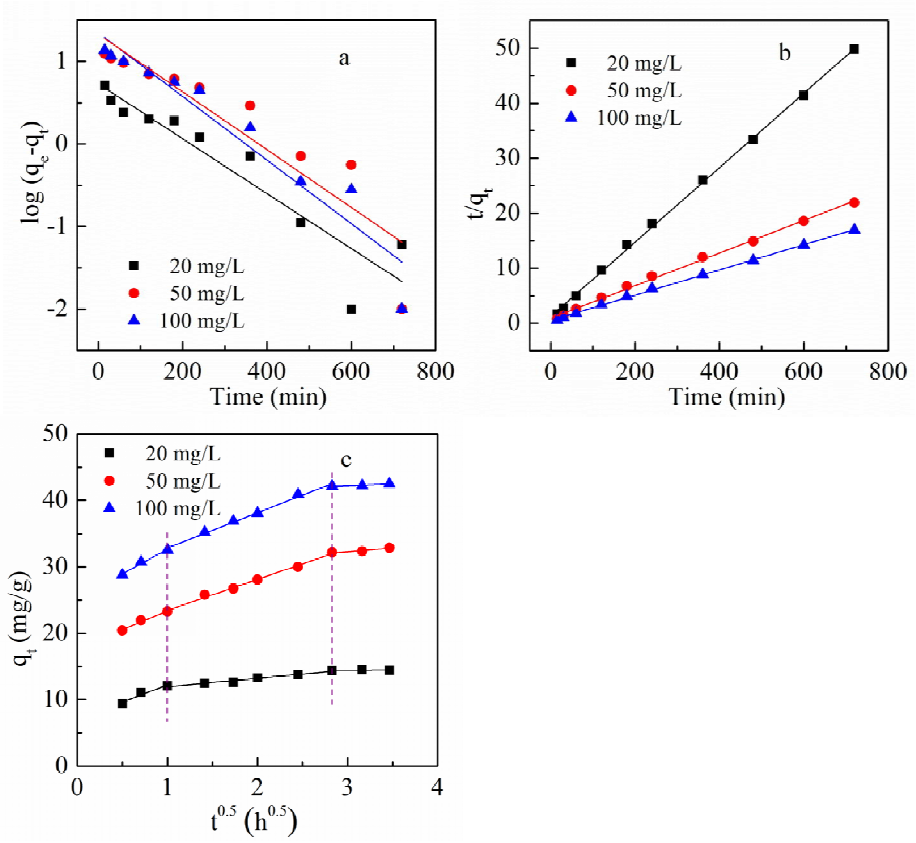


**Fig. 6**

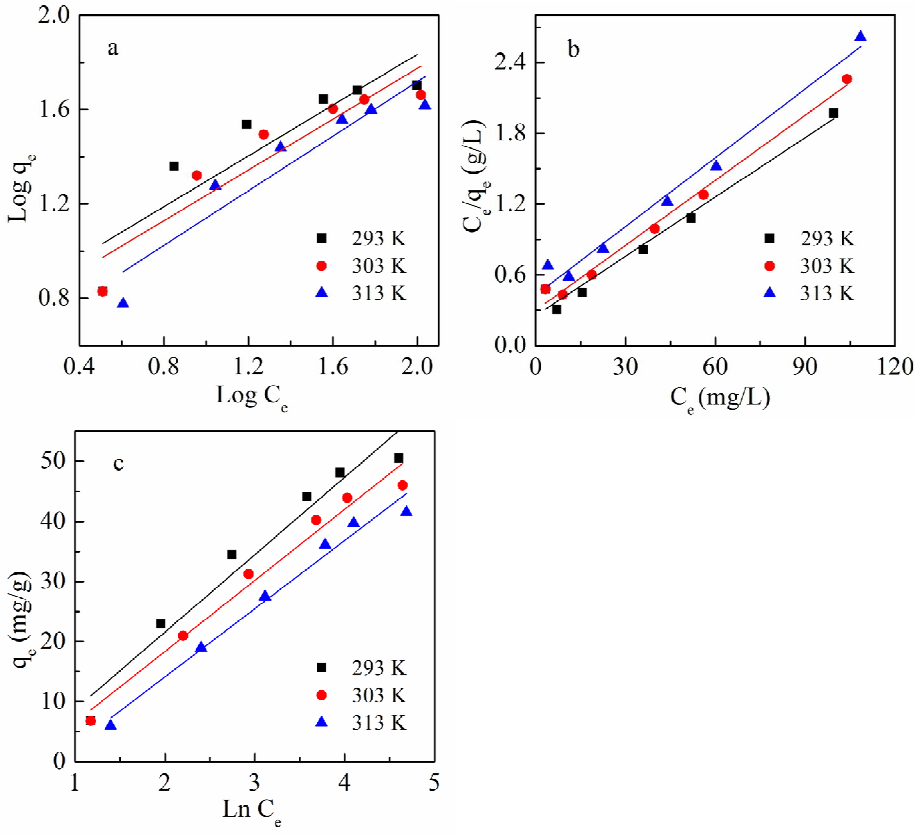


**Fig. 7**

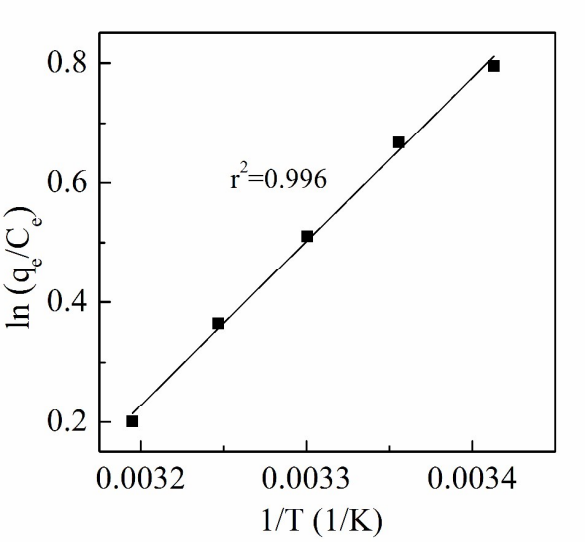


**Fig. 8**

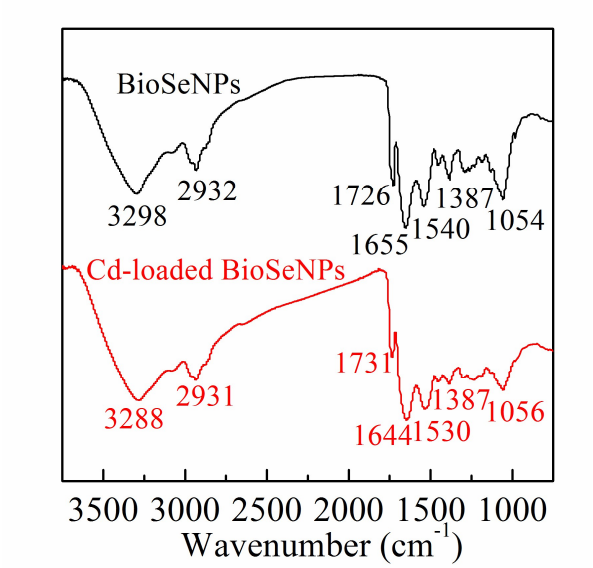


**Fig. 9**

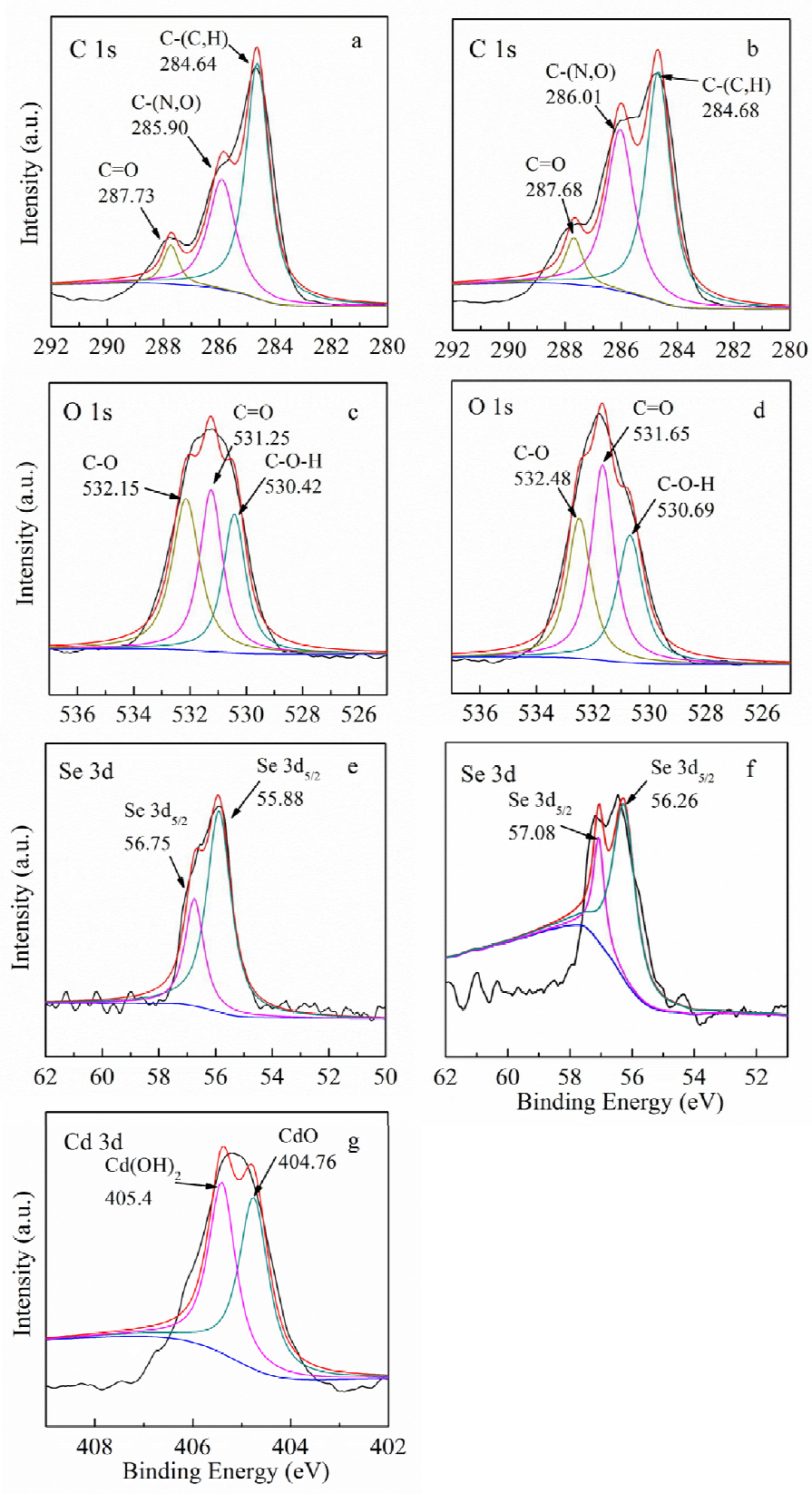


**Fig. 10**

# Tables

**Table 1**

**Pseudo-first-order kinetic parameters for Cd(II) adsorption on BioSeNPs**

| Concentration (mg/L) | $q_{e,exp}$ (mg/L) | Pseudo-first-order | | |
|---|---|---|---|---|
| | | $k_1$ ($\times 10^{-3}$ $s^{-1}$) | $q_{e,cal}$ (mg/L) | $r^2$ |
| 20 | 14.4 | 0.13 | 5.36 | 0.85 |
| 50 | 32.9 | 0.12 | 21.45 | 0.83 |
| 100 | 42.5 | 0.15 | 22.19 | 0.92 |

**Table 2**

**Pseudo-second-order kinetic parameters for Cd(II) adsorption on BioSeNPs**

| Concentration (mg/L) | $q_{e,exp}$ (mg/L) | Pseudo-second-order | | | |
|---|---|---|---|---|---|
| | | $k_2$ ($\times 10^{-4}$ g/ mg s) | $q_{e,cal}$ (mg/L) | h (g /mg s) | $r^2$ |
| 20 | 14.4 | 0.63 | 14.78 | 0.014 | 0.999 |
| 50 | 32.9 | 0.17 | 33.78 | 0.019 | 0.999 |
| 100 | 42.5 | 0.18 | 43.67 | 0.034 | 0.999 |

**Table 3**

**Intra particle diffusion kinetic parameters for Cd(II) adsorption on BioSeNPs**

| Concentration (mg/L) | $K_{id}$ (mg/$g^{-1}$ $h^{0.5}$) | Intercept values (I) | $r^2$ |
|---|---|---|---|
| 20 | 1.28 | 10.67 | 0.96 |
| 50 | 4.67 | 18.80 | 0.99 |
| 100 | 5.30 | 27.55 | 0.99 |

**Table 4**

**Freundlich, Langmuir and Temkin isotherm model parameters and correlation coefficients for adsorption of Cd(II) onto BioSeNPs**

| Isotherm | Temperature (K) | Parameters | | $r^2$ |
|---|---|---|---|---|
| | | $K_F$ | n | |
| Freundlich | 293 | 5.71 | 1.85 | 0.773 |
| | 303 | 4.99 | 1.86 | 0.849 |
| | 313 | 3.70 | 1.73 | 0.861 |
| Isotherm | Temperature (K) | Parameters | | $r^2$ |
| | | $q_m$ (mg/g) | $K_L$ (L/mg) | |
| Langmuir | 293 | 59.70 | 0.066 | 0.971 |
| | 303 | 54.44 | 0.061 | 0.987 |
| | 313 | 51.52 | 0.045 | 0.978 |
| Isotherm | Temperature (K) | Parameters | | $r^2$ |
| | | $K_T$ | b | |
| Temkin | 293 | 0.723 | 12.91 | 0.953 |
| | 303 | 0.639 | 21.08 | 0.972 |
| | 313 | 0.470 | 29.28 | 0.976 |

**Table 5**

**Thermodynamic parameters for adsorption of Cd(II) by BioSeNPs**

| Temperature (K) | $\Delta G^0$ (kJ/mol) | $\Delta H^0$ (kJ/mol) | $\Delta S^0$ (J/mol K) |
|---|---|---|---|
| 293 | -1.94 | -22.75 | -70.91 |
| 303 | -1.29 | -22.75 | -70.91 |
| 313 | -0.52 | -22.75 | -70.91 |

**Table 6**

**Binding energy and relative content of C and O in adsorbents**

| Valence state | Proposed components | Binding energy (eV) | | Relative content% | |
|---|---|---|---|---|---|
| | | BioSeNPs | Cd-loaded BioSeNPs | BioSeNPs | Cd-loaded BioSeNPs |
| C 1s | C-(C,H) | 284.64 | 284.68 | 60.5 | 51.8 |
| | C-(N,O) | 285.90 | 286.01 | 32.8 | 40.7 |
| | C=O | 287.73 | 287.68 | 6.7 | 7.5 |
| O 1s | C-OH | 530.42 | 530.69 | 28.5 | 29.5 |
| | C=O | 531.25 | 531.65 | 33.4 | 40.6 |
| | C-O | 532.15 | 532.48 | 38.1 | 29.9 |

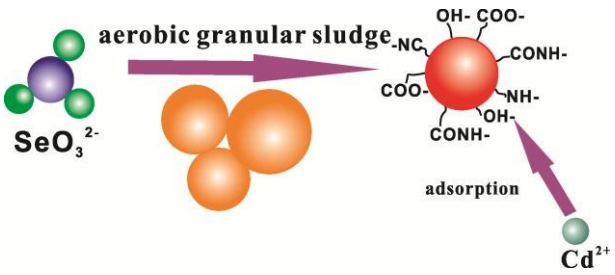


BioSeNPs, which were produced by aerobic granular sludge in a sequencing batch reactor, could be used to remove cadmium from aqueous solution with high efficiency.